

Deformation and recrystallization textures of copper single crystals and bicrystals

SHIOMI KIKUCHI, EIJI KIMURA, MASAHIRO KOIWA

Department of Metal Science and Technology, Kyoto University, Sakyo-ku, Kyoto 606, Japan

Recrystallization textures in rolled copper specimens have been investigated so as to elucidate the mechanisms of cube texture formation. The specimens are single crystals with the orientations corresponding to the main components of the rolled textures, such as $\{112\}\langle 111\rangle$, $\{110\}\langle 112\rangle$, etc. and bicrystals consisting of such oriented crystals. The cube texture was not observed in any single crystal specimens, but observed in only two bicrystal specimens with $\{112\}\langle 111\rangle/\{100\}\langle 001\rangle$ and $\{110\}\langle 112\rangle/\{100\}\langle 001\rangle$ orientations. The formation of cube texture seems to require the existence of a cube oriented region in the deformed state, and the favourable oriented matrix to allow the growth of such nuclei.

1. Introduction

It is well known that the recrystallization texture of face-centred cubic (fcc) pure metals, such as copper and aluminium, shows the simple "cube texture". Although the mechanism of the cube texture formation has been studied extensively [1-5], it is still not yet clear whether the oriented nucleation or the oriented growth dominates the texture formation. Experiments by use of single crystals and bicrystals are considered to shed light on this problem. In such specimens, the deformation structure or texture is simple, and the role of the grain boundary can be studied easily. The crystal orientation relationship between nucleated or grown grains and the matrix can be easily determined by X-ray diffraction or electron channelling pattern.

It has been reported that the rolling textures of fcc pure metals have four main orientation components: $\{123\}\langle 412\rangle$, $\{112\}\langle 111\rangle$, $\{110\}\langle 112\rangle$ and $\{110\}\langle 001\rangle$ [1, 2]. For rolled single crystals with such textures, the orientation after recrystallization anneal can be described by rotations of 30-40° around a common $\langle 111\rangle$ pole of the matrix [1, 2]. Recent works of Gottstein and co-workers [6, 7] and Berger *et al.* [8] have shown that the final grains with the above rotational relationship merge by a sequence of twinning events for metals with low stacking fault energy. These results support the oriented growth theories because high grain boundary mobility in fcc metals is associated with a 30-40° $\langle 111\rangle$ rotation as shown by Kronberg and Wilson [9]. However, there is little experimental evidence to show the strong cube texture in single crystals [10, 11]. On the other hand, Ridha and Hutchinson [4] showed from the oriented nucleation view that in copper polycrystals the recrystallized grains with the cube orientation originate in the regions of transition bands with a rotation axis corresponding approximately to the rolling direction as predicted by Dillamore and Katoh [3]. The exist-

ence of cube oriented deformed cells may develop into recrystallization nuclei by the growing mechanisms such as sub-boundary migration.

Hu [2] has suggested the importance of experiments on bicrystals to clarify the role of interfaces between two texture components. Such experiments have been reported in copper [12] and aluminium [13].

In this investigation the deformation and recrystallization texture near the grain boundary is examined in detail for six kinds of copper bicrystals consisting of the combination of two components among the above four main rolling texture components. For the sake of comparison, the deformation and recrystallization textures are also examined for polycrystals, and single crystals with various orientations.

2. Materials and experimental

Specimens used were copper polycrystal, single crystals and bicrystals of 99.99% purity. Single crystals and some bicrystals were grown using seed crystals in carbon moulds in a vacuum by the Bridgman method. Bicrystals which are difficult to grow by the Bridgman method were prepared by diffusion bonding: two single crystals with electro-polished surfaces were placed between stainless steel plates, fastened with four bolts at the corner, and held at 1263 K in a vacuum for 15 h.

Dimensions of specimens used and the rolling direction, *RD*, are shown in Fig. 1. The grain boundary in the bicrystals was parallel to the rolling direction and the normal direction, *ND*. The orientations of specimens used were:

- (a) single crystals,
 $\{112\}\langle 111\rangle$, $\{110\}\langle 112\rangle$, $\{110\}\langle 001\rangle$,
 $\{123\}\langle 412\rangle$, $\{100\}\langle 001\rangle$;

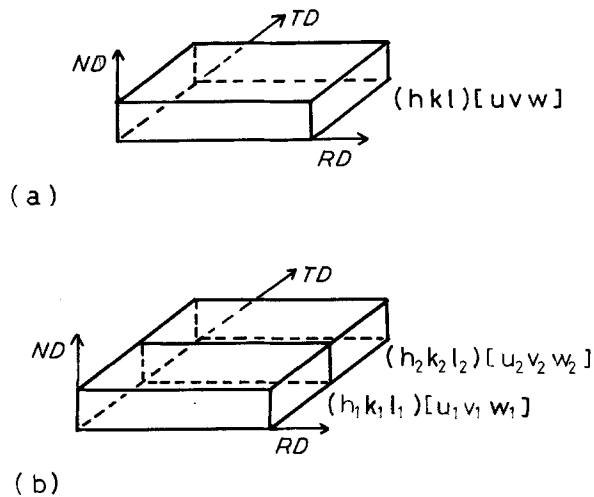


Figure 1 Specimen geometry of (a) a single crystal and (b) a bicrystal.

(b) bicrystals,

$$\begin{aligned} & \{112\} \langle 111 \rangle / \{110\} \langle 112 \rangle, \\ & \{112\} \langle 111 \rangle / \{110\} \langle 001 \rangle, \\ & \{112\} \langle 111 \rangle / \{100\} \langle 001 \rangle, \\ & \{110\} \langle 112 \rangle / \{110\} \langle 001 \rangle, \\ & \{110\} \langle 112 \rangle / \{100\} \langle 001 \rangle, \\ & \{110\} \langle 001 \rangle / \{100\} \langle 001 \rangle. \end{aligned}$$

The orientations of $\{112\} \langle 111 \rangle$, $\{110\} \langle 112 \rangle$, $\{110\} \langle 001 \rangle$ and $\{123\} \langle 412 \rangle$ are the main components of deformation textures for the rolled copper. The $\{100\} \langle 001 \rangle$ orientation rotates into the $\{123\} \langle 412 \rangle$ orientation by heavy rolling.

All the specimens were deformed by rolling to 90% reduction, and then annealed in a vacuum at 773 K. The annealing time was one hour for polycrystals and single crystals, and 30 s for bicrystals. Both the deformation and the recrystallization textures were measured on the X-ray pole figure automatic measurement system (Philips APD 1700 system) by using MoK_α radiation in the Schulz reflection method. The specimens of bicrystals for the pole figure measurement were prepared by piling up five pieces cut along the boundary with 2 mm width to measure the texture only near the grain boundary as shown in Fig. 2. It was ascertained by optical microscopy whether the annealed specimens completed the recrystallization.

3. Results and discussion

3.1. Recrystallization textures of polycrystals

The recrystallization texture is known to be sensitively affected by specimen purity, the degree of deformation and annealing temperature. Therefore, the recrystallization texture of polycrystalline specimens from the same lot as that used for single and bicrystal specimens was examined.

The experimental parameters are as following:

reduction in rolling 80%, 90%;

annealing temperature 573 K, 773 K;

annealing time 1 h.

The cube texture could not be observed for the 80% rolled specimen after annealing at either temperatures. For the 90% rolled specimen, the cube texture was

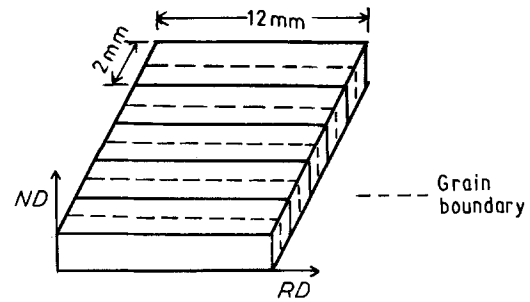


Figure 2 Dimensions of the specimen used for the measurement of textures near the grain boundary in bicrystals.

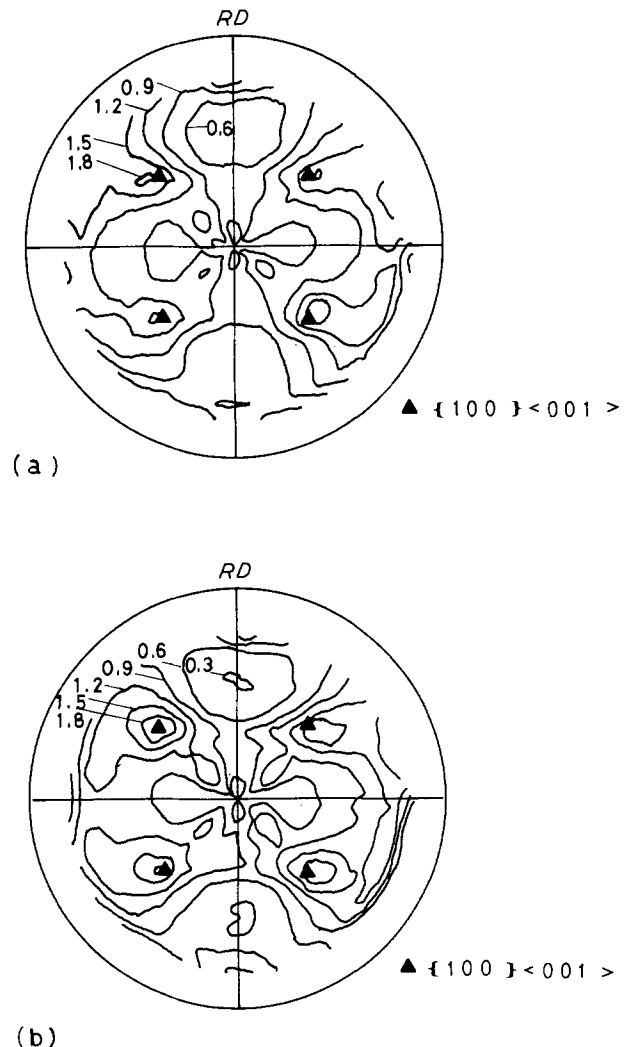


Figure 3 (111) pole figures of the recrystallization textures in copper polycrystalline samples rolled 90% and annealed at (a) 573 K for 1 h and (b) 773 K for 1 h.

clearly observed after annealing at both the temperatures (Fig. 3), but much stronger for the annealing at the higher temperature of 773 K.

Therefore, the experimental conditions of 90% rolling and annealing at 773 K were adopted for the investigation of single crystals and bicrystals.

3.2. Deformation and recrystallization textures of single crystals

Fig. 4a–e shows the deformation textures of single crystals with various orientations after 90% reduction.

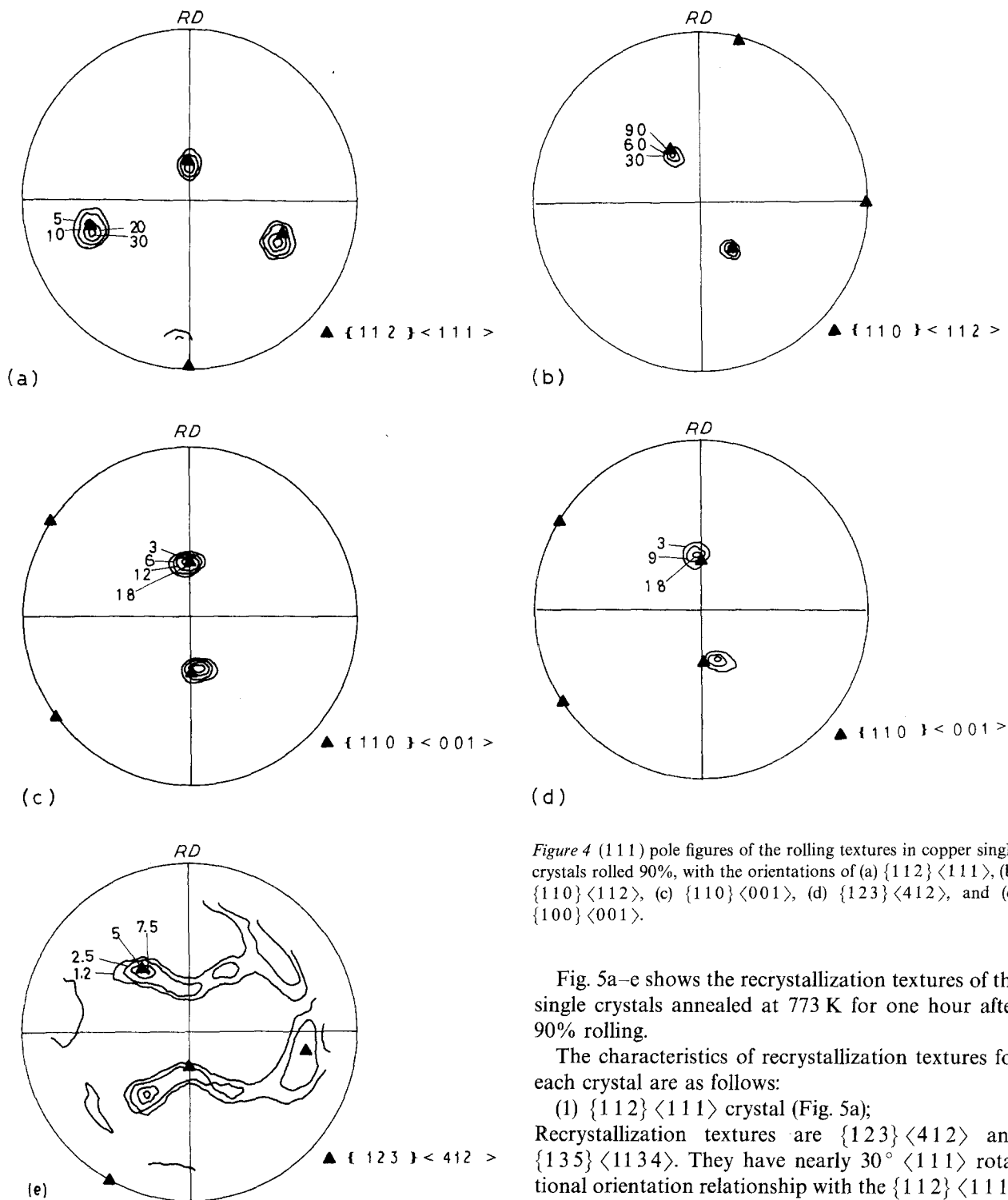


Figure 4 (111) pole figures of the rolling textures in copper single crystals rolled 90%, with the orientations of (a) $\{112\} \langle 111 \rangle$, (b) $\{110\} \langle 112 \rangle$, (c) $\{110\} \langle 001 \rangle$, (d) $\{123\} \langle 412 \rangle$, and (e) $\{100\} \langle 001 \rangle$.

Fig. 5a–e shows the recrystallization textures of the single crystals annealed at 773 K for one hour after 90% rolling.

The characteristics of recrystallization textures for each crystal are as follows:

(1) $\{112\} \langle 111 \rangle$ crystal (Fig. 5a);

Recrystallization textures are $\{123\} \langle 412 \rangle$ and $\{135\} \langle 1134 \rangle$. They have nearly $30^\circ \langle 111 \rangle$ rotational orientation relationship with the $\{112\} \langle 111 \rangle$ matrix.

(2) $\{110\} \langle 112 \rangle$ crystal (Fig. 5b);

Strong $\{144\} \langle 454 \rangle$ and weak $\{110\} \langle 114 \rangle$ textures are formed.

(3) $\{110\} \langle 001 \rangle$ crystal (Fig. 5c);

The $\{112\} \langle 512 \rangle$ recrystallization texture is obtained.

(4) $\{123\} \langle 412 \rangle$ crystal (Fig. 5d);

The $\{125\} \langle 432 \rangle$ texture is the strongest, which is near the initial orientation before deformation. The $\{125\} \langle 432 \rangle$ orientation has approximately the $50^\circ \langle 111 \rangle$ rotational orientation relationship with the deformation texture, $\{110\} \langle 001 \rangle$, derived from the $\{123\} \langle 412 \rangle$ crystal. The $\{025\} \langle 001 \rangle$ and $\{110\} \langle 001 \rangle$ components are also observed. The former is the rotated $\{110\} \langle 001 \rangle$ and the latter is the retained one of the deformed texture.

It is evident from the $\{111\}$ pole figures that the initial orientations before rolling are maintained even after heavy deformation (90% reduction) in the $\{112\} \langle 111 \rangle$, $\{110\} \langle 112 \rangle$ and $\{110\} \langle 001 \rangle$ crystals. These crystals have several equivalent slip systems with respect to the rolling direction and can be deformed with little crystal rotation. The $\{123\} \langle 412 \rangle$ crystal rotates to the $\{110\} \langle 001 \rangle$ orientation by rolling; this orientation is not suitable to obtain the $\{123\} \langle 412 \rangle$ orientation in the deformed state. In contrast, the $\{100\} \langle 001 \rangle$ crystal rotates to the $\{123\} \langle 412 \rangle$ orientation. Therefore, the proper orientations composing the bicrystals should be selected from four orientations of $\{112\} \langle 111 \rangle$, $\{110\} \langle 112 \rangle$, $\{110\} \langle 001 \rangle$ and $\{100\} \langle 001 \rangle$.

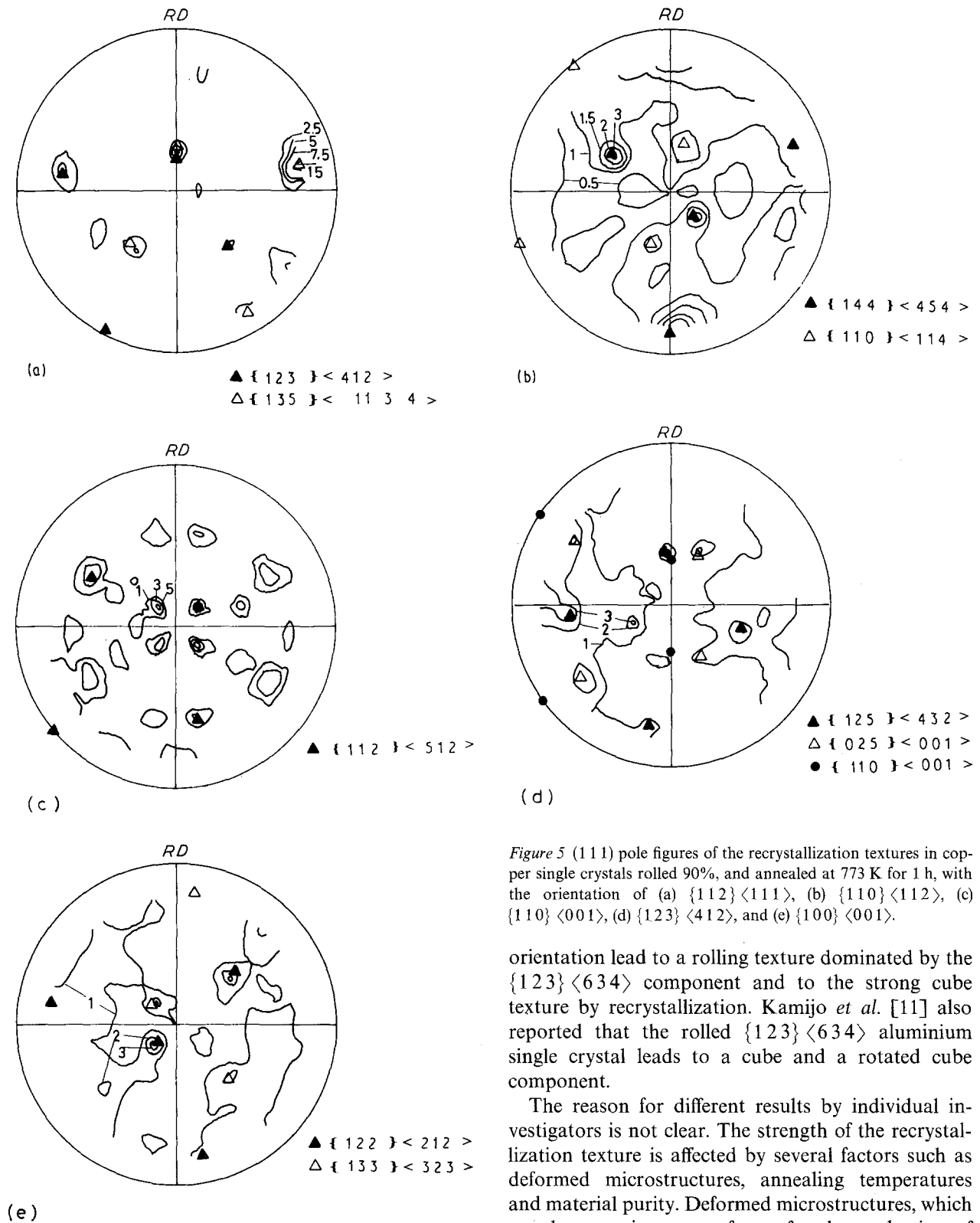


Figure 5 (111) pole figures of the recrystallization textures in copper single crystals rolled 90%, and annealed at 773 K for 1 h, with the orientation of (a) $\{112\} \langle 111 \rangle$, (b) $\{110\} \langle 112 \rangle$, (c) $\{110\} \langle 001 \rangle$, (d) $\{123\} \langle 412 \rangle$, and (e) $\{100\} \langle 001 \rangle$.

orientation lead to a rolling texture dominated by the $\{123\} \langle 634 \rangle$ component and to the strong cube texture by recrystallization. Kamijo *et al.* [11] also reported that the rolled $\{123\} \langle 634 \rangle$ aluminium single crystal leads to a cube and a rotated cube component.

The reason for different results by individual investigators is not clear. The strength of the recrystallization texture is affected by several factors such as deformed microstructures, annealing temperatures and material purity. Deformed microstructures, which are the most important factor for the nucleation of recrystallized grains, are also influenced by the total rolling reduction, the amount of reduction per pass and rolling temperatures. Such details of experimental procedures, usually not specified in papers, seem to be responsible for different results of individual investigation. Within the experimental condition of the present experiment, cube texture was not found for single crystals with various orientations.

3.3. Deformation and recrystallization texture of bicrystals

Fig. 6a–f shows the deformation texture near the grain

(5) $\{100\} \langle 001 \rangle$ crystal (Fig. 5e).

The recrystallization textures obtained are $\{122\} \langle 212 \rangle$ and $\{133\} \langle 323 \rangle$. The $\{122\} \langle 212 \rangle$ orientation is the twin relation with the $\{100\} \langle 001 \rangle$.

These results are summarized in Table I. No cube texture is observed in the recrystallized specimens. In most of studies using single crystals similar results have been reported in the literature [1]. There are a few publications showing the formation of cube texture in single crystals. Kohlhoff *et al.* [10] showed that copper single crystals of $(001) [100]$ and $(111) [110]$

TABLE I Deformation and recrystallization textures of copper single crystals

Specimens	Deformation textures	Recrystallization textures
{112} <111>	{112} <111>	{123} <412>, {135} <1134>
{110} <112>	{110} <112>	{144} <454>, {110} <114>
{110} <001>	{110} <001>	{112} <512>
{123} <412>	{110} <001>	{110}, <001>, {125} <432>, {025} <100>
{100} <001>	{123} <412>	{133} <323>, {122} <212>

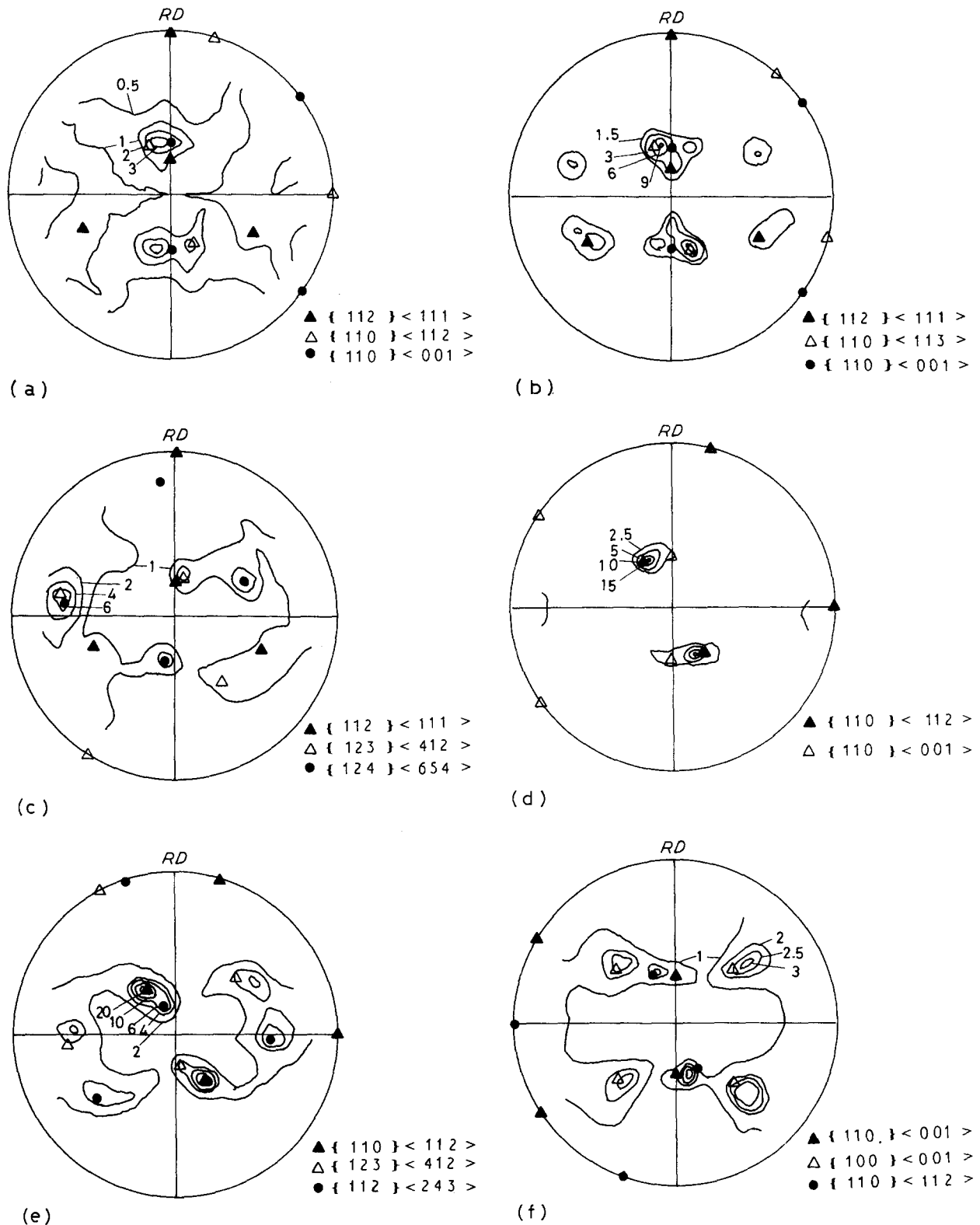


Figure 6 (111) pole figures of the rolling textures in copper bicrystals rolled 90%, with the orientation of (a) {112} <111>/{110} <112>, (b) {112} <111>/{110} <001>, (c) {112} <111>/{100} <001>, (d) {110} <112>/{110} <001>, (e) {110} <112>/{100} <001> and (f) {110} <001>/{100} <001>.

boundary in the rolled bicrystals. Extra texture components, in addition to those observed in the respective single crystal specimens are:

- {110} <001> for the {112} <111>/{110} <112>;
- {110} <113> for the {112} <111>/{110} <001>;
- {124} <654> for the {112} <111>/{100} <001>;

- {112} <243> for the {110} <112>/{100} <001>;
- {100} <001> and {110} <112> for the {110} <001>/{100} <001> crystal.

In these additional components, the {124} <654> and the {112} <243> are the components near the {123} <412> texture which is formed from the {100} <001> single crystal. It should be noted that the {100} <001> component is retained in the

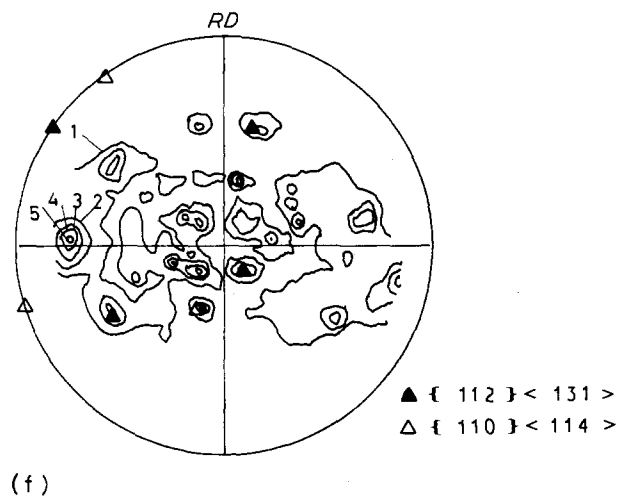
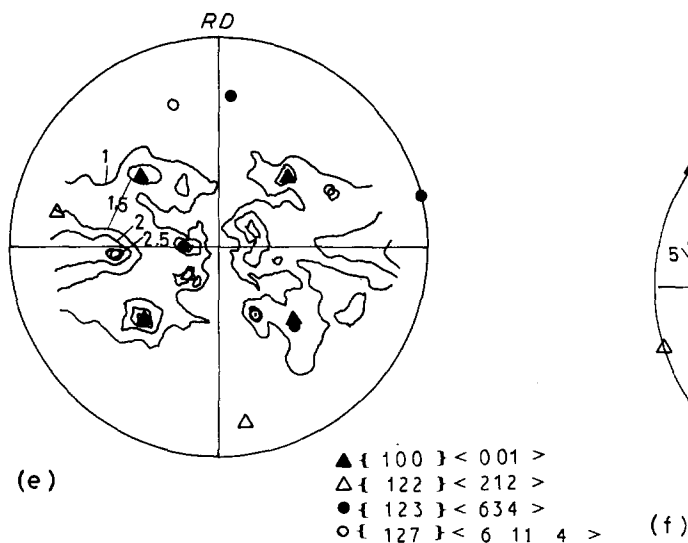
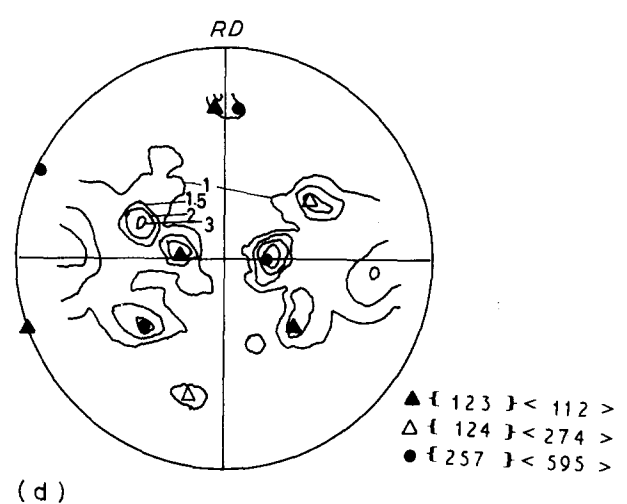
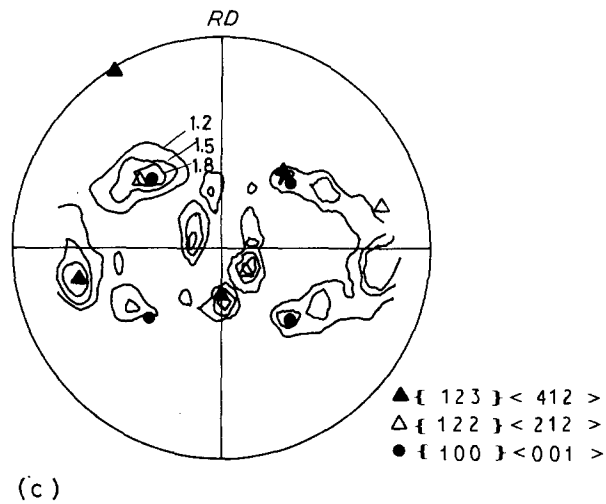
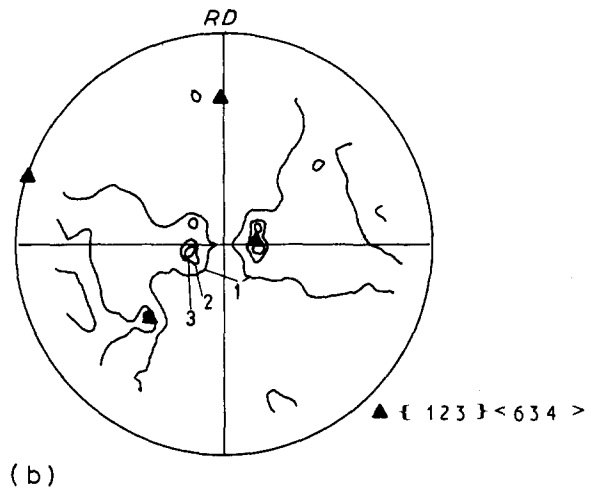
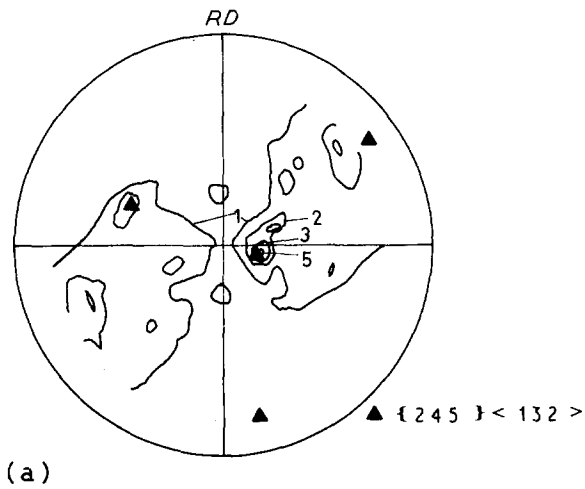


Figure 7 (111) pole figures of the recrystallization textures in copper bicrystals rolled 90%, and annealed at 773 K for 30 s., with the orientations of (a) {112} <111>/{110} <112>, (b) {112} <111>/{110} <001>, (c) {112} <111>/{100} <001>, (d) {110} <112>/{110} <001>, (e) {110} <112>/{100} <001>, (f) {110} <001>/{100} <001>.

$\{110\}\langle 112\rangle/\{100\}\langle 001\rangle$ bicrystal although in the single crystal experiment the $\{100\}\langle 001\rangle$ orientation rotates to the $\{123\}\langle 412\rangle$ by rolling; the grain boundary restrains a crystal rotation during deformation.

The recrystallization textures near the grain boundary of the above bicrystals are shown in Fig. 7a–f. The annealing treatment is performed at 773k for 30s for the 90% rolled specimen. The results are as follows:

(1) $\{112\}\langle 111\rangle/\{110\}\langle 112\rangle$ bicrystal (Fig. 7a); The $\{245\}\langle 132\rangle$ texture is obtained, which is not found in the single crystals with each component.

(2) $\{112\}\langle 111\rangle/\{110\}\langle 001\rangle$ bicrystal (Fig. 7b);

The $\{123\}\langle 634\rangle$ texture is formed, which is often called *R* orientation and one of the main recrystallization textures of copper polycrystals.

(3) $\{112\}\langle 111\rangle/\{100\}\langle 001\rangle$ bicrystal (Fig. 7c); The cube texture is observed, and the $\{123\}\langle 412\rangle$ and $\{122\}\langle 212\rangle$ components are also formed. The $\{122\}\langle 212\rangle$ orientation is a twin orientation of the $\{100\}\langle 001\rangle$ crystal. The $\{123\}\langle 412\rangle$ texture is the same as the deformation texture of the $\{100\}\langle 001\rangle$ single crystal and also the recrystallization texture of the $\{112\}\langle 111\rangle$ single crystal.

(4) $\{110\}\langle 112\rangle/\{110\}\langle 001\rangle$ bicrystal (Fig. 7d);

The recrystallization texture components are the $\{123\}\langle 112\rangle$, $\{124\}\langle 274\rangle$ and $\{257\}\langle 595\rangle$.

(5) $\{110\}\langle 112\rangle/\{100\}\langle 001\rangle$ bicrystal (Fig. 7e); The cube texture is observed again. The other components obtained are the $\{122\}\langle 212\rangle$, $\{123\}\langle 634\rangle$ and $\{127\}\langle 6114\rangle$.

The $\{122\}\langle 212\rangle$ has the twin relationship with the $\{100\}\langle 001\rangle$ as already mentioned. The $\{127\}\langle 6114\rangle$ orientation is approximately the $40^\circ\langle 111\rangle$ rotational orientation with the $\{110\}\langle 112\rangle$ matrix.

(6) $\{110\}\langle 001\rangle/\{100\}\langle 001\rangle$ bicrystal (Fig. 7f); The $\{112\}\langle 131\rangle$ and $\{110\}\langle 114\rangle$ components are observed. The $\{110\}\langle 114\rangle$ component is the

rotational relationship of the $\{110\}\langle 001\rangle$ about *RD* axis.

These results of deformation recrystallization textures are summarized in Table 2.

3.4. Formation of cube texture

In the present experiment, the cube texture components are observed only in two bicrystal specimens: $\{112\}\langle 111\rangle/\{100\}\langle 001\rangle$ and $\{110\}\langle 112\rangle/\{100\}\langle 001\rangle$.

There are two principal mechanisms for the nucleation of recrystallization textures in fcc metals [2, 8]. One is the nucleation with orientation components present in the deformed matrix, followed by repeat growth accidents that form annealing twins. The twinning sequence ceases when an orientation is favourable for the growth, that is the well-known $30\text{--}40^\circ\langle 111\rangle$ orientation relationship. The other is the nucleation and growth with orientation components existing in the deformed matrix.

In the present investigation the bicrystals showing the cube texture have the $\{123\}\langle 412\rangle$ deformation texture after rolling. Kohlhoff *et al.* [13] have reported that in copper single crystals the cube texture is generated from the $\{123\}\langle 634\rangle$ component by twin formation. The cube orientation has the $40^\circ\langle 111\rangle$ orientation relationship with the $\{123\}\langle 634\rangle$ deformed component. In this experiment of single crystals, recrystallization textures having the $\langle 111\rangle$ rotational relationship with the deformed matrix are often observed. However, the $\{100\}\langle 001\rangle$ single crystal having the $\{123\}\langle 412\rangle$ deformation texture which is close to the $\{123\}\langle 643\rangle$ never shows cube texture. Therefore, it is difficult to consider that the cube texture observed in the above experiment in bicrystals is generated by only the twin chain mechanism.

Among the six bicrystal specimens used in this experiment, the cube texture was formed in two specimens, both of which had the $\{100\}\langle 001\rangle$ crystal as one of the components. Although this component has

TABLE II Deformation and recrystallization textures near the grain boundary of copper bicrystals

Specimens	Deformation Textures	Recrystallization Textures
$\{112\}\langle 111\rangle/\{110\}\langle 112\rangle$	$\{112\}\langle 111\rangle$ $\{110\}\langle 112\rangle$ $\{110\}\langle 001\rangle$	$\{245\}\langle 132\rangle$
$\{112\}\langle 111\rangle/\{110\}\langle 001\rangle$	$\{112\}\langle 111\rangle$ $\{110\}\langle 001\rangle$ $\{110\}\langle 113\rangle$	$\{123\}\langle 634\rangle$
$\{112\}\langle 111\rangle/\{100\}\langle 001\rangle$	$\{112\}\langle 111\rangle$ $\{123\}\langle 412\rangle$ $\{124\}\langle 654\rangle$	$\{123\}\langle 412\rangle$ $\{122\}\langle 212\rangle$ $\{100\}\langle 001\rangle$
$\{110\}\langle 112\rangle/\{110\}\langle 001\rangle$	$\{110\}\langle 112\rangle$ $\{110\}\langle 001\rangle$	$\{123\}\langle 112\rangle$ $\{124\}\langle 274\rangle$ $\{257\}\langle 595\rangle$
$\{110\}\langle 112\rangle/\{100\}\langle 001\rangle$	$\{110\}\langle 112\rangle$ $\{123\}\langle 412\rangle$ $\{112\}\langle 243\rangle$	$\{100\}\langle 001\rangle$ $\{122\}\langle 212\rangle$ $\{123\}\langle 634\rangle$ $\{127\}\langle 6114\rangle$
$\{110\}\langle 001\rangle/\{100\}\langle 001\rangle$	$\{110\}\langle 001\rangle$ $\{100\}\langle 001\rangle$ $\{110\}\langle 112\rangle$	$\{112\}\langle 131\rangle$ $\{110\}\langle 114\rangle$

rotated to the $\{123\}\langle 412\rangle$ after rolling and the $\{100\}\langle 001\rangle$ cannot be detected by X-ray measurement, it is possible that some residue remains near the grain boundary, which might act as the nuclei for the cube texture formation on recrystallization. Then one might wonder why the other bicrystal specimen with $\{100\}\langle 001\rangle$ failed to develop the cube texture. In this specimen the recrystallization texture near the grain boundary is similar to that obtained in the $\{110\}\langle 001\rangle$ single crystal. It seems that the recrystallized grains in the $\{110\}\langle 001\rangle$ side grew preferentially into the $\{100\}\langle 001\rangle$ side.

Thus the cube texture is considered to be formed when

(1) there exist cube oriented regions or nuclei in the deformed matrix, and

(2) the matrix around the nuclei is a favourable orientation for the growth of the nuclei.

Direct observation of grain boundaries of bicrystal specimens by electron microscopy is expected to give a clear answer to this inference; such experiments are in progress.

4. Conclusions

The recrystallization textures of copper single crystals and bicrystals have been investigated in X-ray pole figure measurements. The following results were obtained.

1. Cube texture was not found in single crystals with the orientations of main deformation texture components in copper polycrystals.

2. For bicrystal experiments, the nucleation of cube texture can be observed near the grain boundary in only two specimens of the $\{112\}\langle 111\rangle/\{100\}\langle 001\rangle$ and $\{110\}\langle 112\rangle/\{100\}\langle 001\rangle$ bicrystals.

3. The formation of cube texture requires the cube component in the deformed matrix. In addition, the matrix around the cube nuclei must be favourable in orientation for the growth.

Acknowledgement

The authors thank Prof. K. Ono, Dr. R. O. Suzuki and Mr. M. Hamura for the use of X-ray instruments, Dr. K. Ikeuchi, Osaka University, for his helpful suggestion on the diffusion bonding, and Mr. H. Shirai, Mitsubishi Cable Industries Ltd, for supplying the materials.

References

1. P. A. BECK and H. HU, "Recrystallization, Grain growth and Textures" edited by H. Margolin (ASM, Metals Park, Ohio 1966) p. 393
2. H. HU, "Annealing Processes—Recovery, Recrystallization and Grain Growth" in 7th Risø International Symposium, 1986 p. 75
3. I. L. DILLARMORE and H. KATOH, *Metal Sci.* **8** (1974) 73
4. A. A. RIDHA and W. B. HUTCHINSON, *Acta Met.* **26** (1978) 61
5. J. HJELEN and E. NES, "Annealing Processes—Recovery, Recrystallization and Grain Growth" in 7th Risø International Symposium, 1986 p. 367
6. G. GOTTSTEIN, D. ZABARDJADI and H. MECKING, *Met. Sci.* **13** (1979) 223
7. G. GOTTSTEIN, *Acta Met.* **32** (1984) 1117
8. A. BERGER, P. J. WILBRANDT, F. ERNST, V. KLEMENT and P. HASSEN, "Progress in Materials Science, **32** (1988) 1
9. M. L. KRONBERG and F. H. WILSON, *Trans. AIME* **185** (1949) 501
10. G. D. KOHLHOFF, B. KRENTSCHER, W. WANG and K. LÜCKE, "Annealing Processes—Recovery, Recrystallization and Grain Growth" in 7th Risø International Symposium, 1986.
11. T. KAMIJO, A. FUJIWARA and Y. YONEDA, *Keikinzoku* **40** (1990) 906 (in Japanese)
12. H. W. F. HELLER, C. A. VERBRAAK and B. H. KOLSTER, *Acta Met.* **32** (1984) 1395
13. S. KIKUCHI, S. KUDO, M. ODA and M. KOIWA, *J. Mater. Sci. Let.* **9** (1990) 1152

Received 14 May

and accepted 20 September 1991